〈Original article〉

# Comparative structure analysis of tyramine-β-hydroxylase from fruit fly and ADME/T-based profiling of 1-arylimidazole-2 (3*H*)-thiones as potential inhibitors

Md. Nazmul Hasan[1, 2], Arafat Rahman Oany[3], Akinori Hirashima[1,*]

**Summary**  Tyramine-β-hydroxylase (TβH) converts tyramine to octopamine, a neurotransmitter present in insects similar to norepinephrine in mammals. The amino acid sequence of this enzyme is homologous to that of dopamine-β-hydroxylase (DβH). The amino acids sequence of TβH from *Drosophila melanogaster* (DmTβH) is highly similar (56.3%) with African malaria mosquito *Anopheles gambiae* whereas 41.9% protein similarity was found with human DβH. In this study, the 3D structure of DmTβH was predicted using 2 homology based predpiction servers: MODELLER and Phyre2. The homology structures were evaluated and stereo-chemical analyses were done by Ramachandan plot analysis. Validation of these homology models by Ramachandan plot revealed that MODELLER generated model was comparatively better than that of the Phyre2. Additionally. It was found that 1-[4-(trifluromethyl)phenyl]-1,3-dihydro-2*H*-imidazole-2-thione binds to the protein with a binding energy value -10.4 (Kcal/mol) and showed a drug likeness activity with no predicted health hazards. It can be used as a potent inhibitor of DmTβH to design effective pesticide in future after advanced evaluation.

**Key words:** Phylogenic analysis, *Drosophila melanogaster* tyramine-β-hydroxylase (DmTβH), homology modeling.

## 1. Introduction

Tyramine-β-hydroxylase (TβH) converts tyramine (TA) to octopamine (OA), a neurotransmitter present in insects similar to norepinephrine in mammals. OA and TA are biogenic amines exist specially in insect's nervous system and act as a neurotransmitter, neuromodulator and neurohormone in many physiological processes including carbohydrate metabolism, reproduction, oviposition, muscle contraction, locomotion and excretion[1-9]. TA is

[1]Laboratory of Pesticide Chemistry, Division of Molecular Biosciences, Department of Bioscience and Biotechnology, Faculty of Agriculture, Kyushu University, 6-10-1 Hakozaki, Fukuoka 812-8581, Japan
[2]Department of Genetic Engineering and Biotechnology, Jessore University of Science and Technology, Jessore-7408, Bangladesh

[3]Department of Biotechnology and Genetic Engineering, Mawlana Bhashani Science and Technology University, Santosh, Tangail-1902, Bangladesh

utilized as a biosynthetic precursor of OA. TβH hydroxylate TA to generate OA which is involving in a various important physiological functions such as feeding, walking, mating and sting behavior of honeybees, modulation role in flight activity and fight response of locusts, constriction of ovary muscle in fruit flies and locusts, learning, memory, metamorphosis and modulating the activity of juvenile hormone esterase in *Tribolium freemani*, production of light in fireflies, metabolism of carbohydrates, regulating sex pheromone production in *Bombyx mori* and foraging behavior in honeybees[10-20].

A very little information is available about TβH structure and its activity in insects. For the first time, we generated a 3D structure of fruit fly *Drosophila melanogaster* TβH (DmTβH) enzyme using Phyre2 web server based on Phyre2 remote homologous template, Peptidylglycine α-hydroxylating monooxygenase (PHM) crystal structure (PDB ID: 1OPM). Although the model was acceptable, it was not high quality model based on Ramachandan plot analysis due uncovering all 670 amino acid residues of DmTβH. So, our study aim was to develop a high quality 3D model of DmTβH based on combined template (PHM and IVF) by using a different software MODELLER, since no crystallographic structure or good quality 3D structure was reported up to date. It is already reported that TβH is similar with dopamine-β-hydroxylase (DβH) that converts dopamine (DA) to epinephrine (NE) in mammals as because of having common co-substrate ascorbic acid and oxygen for activity[21]. It is already published

that 1-(thienylalkyl)imidazole-2(3*H*)-thiones acts as a potent competitive inhibitors of DβH[22]. 1-arylimidazole-2(3*H*)-thiones (AITs) were found to be a potent inhibitor of DmTβH in our previous *in vitro* study. Based on the highest *in vitro* inhibitory activity of AITs against cloned DmTβH, a training set of compounds was selected for docking and ADME analysis to comprehend the binding interactions and drug likeness activity.
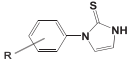
## 2. Materials and Methods

2.1. Selection of a training set of compounds

Among the 30 compounds, 3 compounds: 2-Me-AITs, 4-CF$_3$-AIT and 2-Me,4-Cl-AIT were chosen based on the highest inhibitory activity (*in vitro*) for docking with the newly predicted model and thereafter ADME analysis (Table 1). Selected compounds were prepared by the condensation of the corresponding arylisothiocyanates with aminoacetaldehyde dimethyl acetal followed by acid-catalyzed cyclization of the intermediate *N*-arylthioureas[23, 24]. The 2D structure of the selected compounds was drawn by ChemDraw (ChemDraw Std 13.0) and formatted as .mol files for docking and ACD/L analysis (Fig. 1).

2.2. Homology search and pairwise alignment

Homology search of DmTβH was performed in NCBI blast search from all databases. The amino acid sequences (NCBI accession number NP_78884.1) were aligned in pair to see the pairwise alignment score among homologous organisms[25].

Table 1 Inhibitory activity of training set of AITs against the cloned DmTβH (nM scale) *in vitro* based on highest ID$_{50}$ Value.

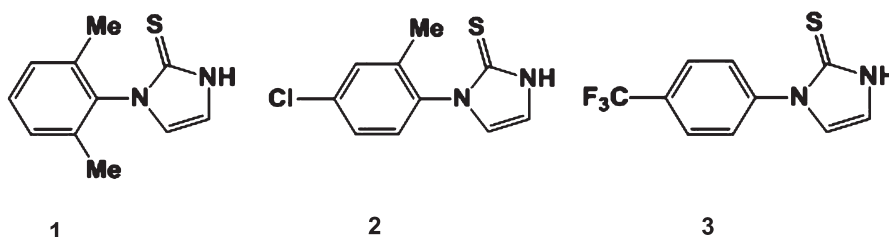| Compound | | | | |
|---|---|---|---|---|
| No. | | R | ID$_{50}$ (nM) | 95% confidence limit (nM) |
| **1** | | 2,6-Me$_2$ | 0.020 | 0.001-0.093 |
| **2** | | 2-Me,4-Cl | 0.154 | 0.053-0.336 |
| **3** | | 4-CF$_3$ | 0.235 | 0.084-0.507 |

Fig. 1. 2D structure of the training set compounds drawn by ChemDraw 13.0.

### 2.3. Phylogenetic analysis

The sequence of DmTβH was multiple-aligned with TβH derived from other organisms including higher animals to insect species using blast search and molecular phylogenetic (neighbor-joining) tree was constructed using Phylogeny fr.[26, 27].

### 2.4. Structural evaluation and molecular docking of DmTβH

Homology model of the conserved region was obtained by MODELLER 9v7 for generating 3D model[28]. A combined template was made based on the best e-value and sequence identity using Maestro Combiguide (version 4.0.)[29]. Subsequently, homology modeling was carried out for DmTβH on the basis of the template using MODELLAR 9v7. The predicted model assessed by PROCHECK server of the SWISS-MODEL Workspace[30, 31]. The reliability test of the secondary and tertiary structure agreement by plotting of the amino acid was performed in Ramachandran plot.

We have already reported a set of compound AITs that interact with the TβH protein *in vitro* (data not shown). Among them, 3 compounds were selected based on highest $ID_{50}$ value for docking to visualize the interaction of protein and small molecules. Autodock Vina was utilized for the performance of molecular docking[32]. The grid box (Centre X: 21.0727, Y: 15.4938, Z: 53.0912 and dimensions (Angstrom): X: 33.0782, Y: 56.2417, Z: 33.6042) was set to cover the entire protein and to execute the blind docking where the compounds are likely to bind in the energetically most suitable portion of a protein. For the visualization of all the protein data files of this study, visualization tool PyMOL molecular graphic system (http://www. pymol.org) was used.

### 2.5. Drug-likeness and ADME/T-based screening

Lipinski's rule of ligands properties and ADMET (absorption, distribution, metabolism, elimination and toxicity) analysis of training set of compounds were carried out to see the drug-likeness activity. Only the compounds that in line with Lipinski's rule, having desired predicted activity and good ADMET properties could be considered for advanced study as pharmacophore modeling or lead identification tests in future.

## 3. Results and Discussion

### 3.1. Pairwise alignment

Pairwise alignment was done between DmTβH and human DβH including others organisms using the accession number (NP_78884.1) in NCBI. Blast searching showed the highest similarity 56.3% in protein and 57.0% in DNA with Agap_AGAp010485 from *Anopheles gambiae*, whereas 41.9 % protein and 52.5 % DNA similarities with human DβH (Table 2).

### 3.2. Phylogenetic analysis

The phylogenetic analysis of DmTβH (Fig.2) shows the major divisions of the DmTβH protein, including insects and other animals. These results suggest that the DmTβH is closely related to insects TβH than to animal TβH.

### 3.3. Structural evaluation and docking study of DmTβH

The DmTβH protein is composed of 670 amino acids as found from GenBank. In MODELLER combined template was prepared by merging with

Table 2  Pairwise alignment score of DmTβH versus other related organisms in database
of NCBI.

| Gene | | Identity (%) | | |
| Species | Symbol | Protein | DNA | Source |
| --- | --- | --- | --- | --- |
| *D. melanogaster* vs. | Tbh | | | |
| *H. sapiens* | DBH | 41.9 | 52.5 | Blast |
| *P. troglodytes* | DBH | 41.9 | 52.6 | Blast |
| *M. mulatta* | DBH | 42.8 | 54.5 | Blast |
| *C. lupus* | DBH | 40.8 | 52.7 | Blast |
| *B. taurus* | DBH | 42.5 | 53.3 | Blast |
| *M. musculus* | Dbh | 41.9 | 53.0 | Blast |
| *R. norvegicus* | Dbh | 40.2 | 51.7 | Blast |
| *G. gallus* | DBH | 42.0 | 51.8 | Blast |
| *X. tropicalis* | dbh | 41.3 | 50.2 | Blast |
| *D. rerio* | dbh | 43.3 | 52.5 | Blast |
| *A. gambiae* | Agap_AGAp010485 | 56.3 | 57.0 | Blast |
| *C. elegans* | Tbh-1 | 42.1 | 50.8 | Blast |
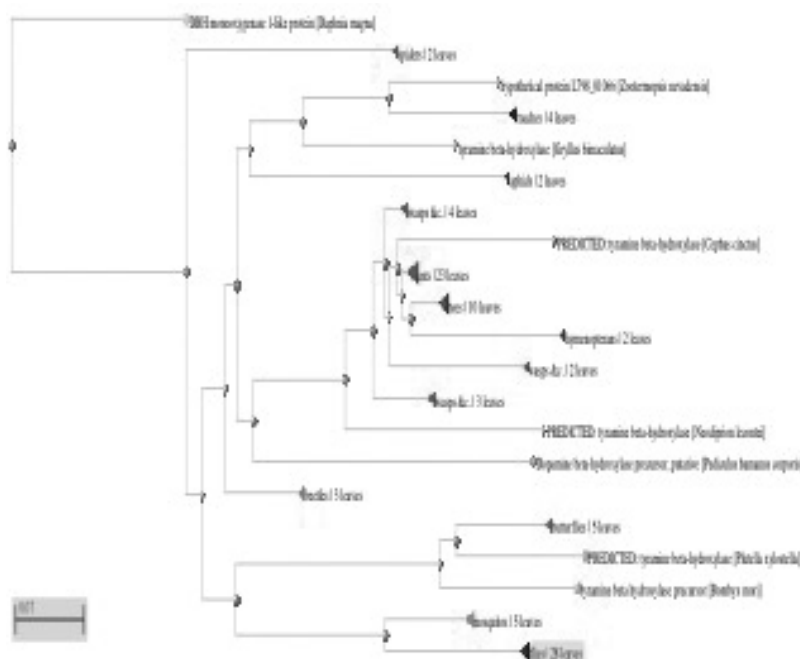


Fig. 2.  Phylogenetic tree of 20 TβH family sequences. Distant analysis of amino acid sequences was performed using the Phylogeny fr. and used as input for neighbor joining tree construction. Sequences were obtained from the GenBank database.

peptidylglycine α-hydroxylating monooxygenase (PHM) (PDB ID: 1OPM) of *Rattus norvegicus* and ethylbenzene dehydrogenase (PDB ID: 2IVF) from *Aromatoleum aromaticum*. A suitable template was made for DmTβH model[33]. Blast searching was performed to select templates for modeling of DmTβH. The combined template was subjected to develop a 3D model of DmTβH. The query and template sequence identity is 30 % and sequence coverage is 50%, with the best e-value in the

PSI-BLAST output. Although sequence identity was still low, it was sufficient for protein modeling[34].

DmTβH amino acid sequences and template pdb file (protein data file) used as input for MODELLER 9v7. MODELLER creates a structural alignment of the query and template and subsequently builds a model on the basis of the homology with the template. The final structure was a pdb file, which was visualized and represented by PyMOL graphic system and domain-wise colored ribbon

image was generated from PyMOL (Fig. 3).

The final model was validated by Ramachandran plot. Ramachandran plot, which calculates the Phi and Psi angles of protein folding and plots accordingly to determine the reliability of the spatial arrangement of the amino acids, results 219 (78.8%) residues were in most favored region out 323 residues in total in PHYRE generated model, whereas model generated by MODELLER showed
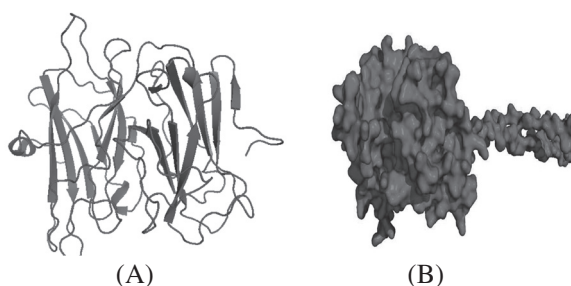


(A)                    (B)

Fig. 3.  Predicted homology modeling of DmTβH generated by Phyre2 based on single template (A) and by MODELLAR 9v2 based on combined template visualized by PyMOL.
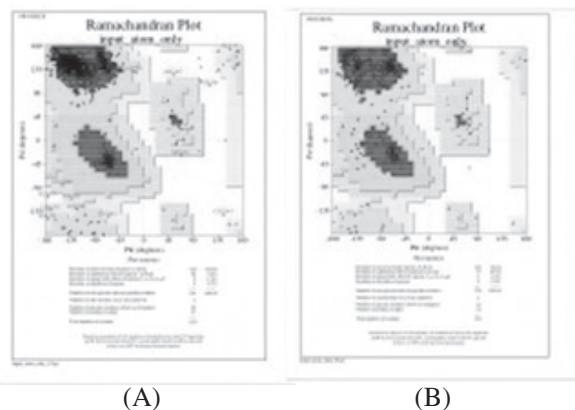


(A)                    (B)

Fig. 4.  Comparative analysis of proposed protein model validation by Ramachandran Plot: Calculation of the psi/phi angle distribution of the model by MODELLER (A) and by Phyre2 (B) as computed by PROCHECK.

520 residues (88.0%) in most favored region out of 670 residues in total (Fig. 4). Amino acids residues are almost 50% decreased in additional allowed region (9.8%) in case of new model compare to previous one. Due to covering all 670 residues, an extended loop was found in newly generated model.

In order to understand the binding mode, selected training set of compounds were docked to the 3D structure of DmTβH. The active domain of the newly generated model was determined the CASTp server[35, 36] (Fig. 5). AutoDock Vina was performed using grid volume covering the entire 3D area of the protein for docking and calculating the free energy value. AutoDock Vina generated different poses of the docked peptide and the best one was picked for the final calculation at RMSD (Root Mean Square Deviation) value of 0.0 (Table 3). The docking interface was visualized with the PyMOL molecular graphics system. The docking study showed that the conformation of the compound (3) with target protein DmTβH has a binding energy of -10.4 (Kcal/mol). It was concluded to be the best docked ligand molecule compare to other two
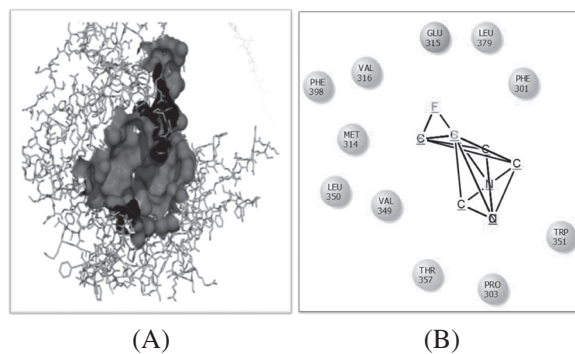


(A)                    (B)

Fig. 5.  (A): The active domains (red in color) of the developed model determined by CASTp server, (B): Responsible amino acids residues for binding and interacting with ligands.

Table 3  Binding energy value and calculation of RMSD by docking analysis.

| Compounds No. | Binding energy (Kcal/mol) | RMSD |
|:---:|:---:|:---:|
| 1 | -7.9 | 0.0 |
| 2 | -8.2 | 0.0 |
| 3 | -10.4 | 0.0 |

molecules. The best suitable binding pocket of the protein for the ligand was determined (Fig. 6) and interacting amino acid residues were found such as Glu 315, Leu 379, Phe 301, Trp 351, Pro 303, Thr 357, Val 349, Leu 350, Met 314, Phe 398, and Val 316. Protein ligand complex of compound no. (1) having highest $ID_{50}$ value (0.020 nM) in *in vitro* experiments have been shown (Fig. 7). In our previous study, we got two suitable pockets for binding with small molecules and the amino acids that consistently involved in the first binding site are Pro339, Arg340, Glu419, Gly332 and Pro338, whereas for the second binding site Pro339, Arg340, Phe530, Leu418, and Pro338.
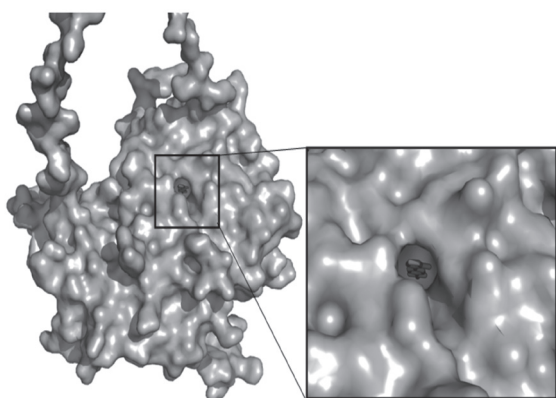
### 3.4. Drug-likeness and ADMET analysis

ADMET analysis plays an important role in drug design. The pharmacokinetic features of the ligand taken into consideration in this work were preliminary investigation. Some properties including human intestinal absorption, blood barrier penetration level, aqueous solubility levels, oral bioavailability and genotoxicity hazards of the selected compounds were analyzed. The use of *in silico* methods to predict ADME properties is intended as a first step and the results of this analysis are herein reported and discussed. The molecular properties of the all three compounds were predicted using ACD/Labs I-lab 2.0 were found to be in accordance with the Lipinski's " Rule of 5" properties,



Fig. 6.  Protein ligand complex: binding interaction between DmTβH and 1-[4-(trifluromethyl) phenyl]-1,3-dihydro-2*H*-imidazole-2-thione. Used docking gridbox: Centre X: 21.0727, Y: 15.4938, Z: 53.0912 and dimensions (Angstrom): X: 33.0782, Y: 56.2417, Z: 33.6042. The highlighted position are binding pocket of the protein, whereas red indicates the ligand molecule.



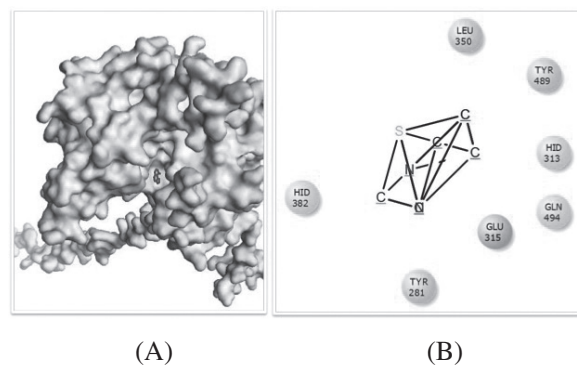(A)                                  (B)

Fig. 7.  Protein ligand complex: binding interaction between DmTβH model and compound no. (1). The highlighted position are binding pocket of the protein (A), whereas red indicates the ligand molecule and responsible amino acids residues for binding and interacting with ligands (B).

Table 4  Ligand's properties analysis.

| Properties/ Compounds No. | 1 | 2 | 3 |
|---|---|---|---|
| Mw | 191.98 | 214.95 | 244.24 |
| Log*P* | 2.511 | 2.696 | 2.818 |
| A log*P* | 1.55 | 1.47 | 1.56 |
| HBA | 2 | 2 | 2 |
| HBD | 1 | 1 | 1 |
| Acid group (no.) | 0 | 0 | 0 |
| TPSA | 35.33 | 35.33 | 47.36 |
| Lipinski's rule violation | 0 | 0 | 0 |
| BBB rule violation | 0 | 0 | 0 |

Table 5  Docking and ADME properties of the training set compounds.

| Ligand properties/Compound No. | Compound's No. | | |
|---|---|---|---|
| | (1) | (2) | (3) |
| Docking energy (Kcal/mol) | -7.9 | -8.2 | -10.4 |
| Number of rotatable bonds | 1 | 1 | 2 |
| Oral bioavailability | > 70% | > 70% | > 70% |
| LogPS | -1.4 | -1.4 | -1.4 |
| LogPB | 0.3 | 0.15 | -0.3 |
| Blood brain barrier (BBB) | Sufficient | Sufficient | Sufficient |
| Fraction unbound in plasma | 0.40 | 0.2699 | 0.1027 |
| Solubility (LogSw) | -3.03 | -3.54 | -3.09 |
| First pass metabolism | No | No | No |
| Stability | pH <2 | pH <2 | pH <2 |
| Passive absorption | > 70% | > 70% | > 100% |

which states that most "drug-like" molecules have $\log P \leqq 5$, molecular weight $\leqq 500$, number of hydrogen bond acceptors $\leqq 10$ and the number of hydrogen bond donors $\leqq 5$[37]. The bioactivities of the selected ligands were predicted using ACD/Labs I-Lab (Tables 4 and 5). Oral bioavailability was found more than 70%, whereas blood barrier penetration sufficient for CNS activity and significant first pass metabolism in liver and/or intestine in case of all tested compounds. The ligands also showed clinically stable (pH < 2) at acidic condition and Passive absorption across intestinal barrier was good (70%-100%).

However, 4-CF$_3$-AIT (3) was the best for drug design considering all docking and ADMET analysis in this study, but it showed the third highest activity in vitro experiments, which means in slico data also support the wet lab data (data not yet published). Furthermore, possible health effects of compound 4-CF$_3$-AIT over blood, cardiovascular system, gastrointestinal system, kidney, liver and lungs were determined by ACD/Labs I-Lab (Algorithm version: v5.0.0.184). The fragmental contribution maps illustrate the role of individual atoms and fragments of the ligand molecule in a color-coded manner; red indicates toxic action whereas green color means negative coefficient in the regression equation that is unrelated to the health effects under investigation (Fig. 8). These estimate are based on data from over 100,000 compounds from chronic, sub-chronic and

acute toxicity and carcinogenicity studies with specific to particular organ systems. Assessment of the safety of new active compounds required the information from different sources as in silico, in vitro, and in vivo. Therefore, it is more likely that in the future, performing the in vivo test using 4-CF$_3$-AIT would give promising results as no genotoxicity hazards was found against hERG inhibitor (Ki < 10
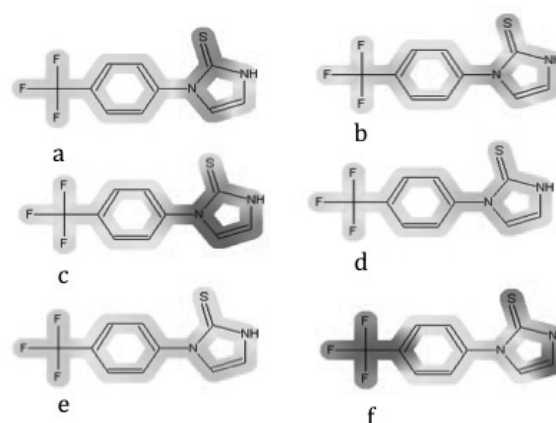


Fig. 8.  The fragmental contribution maps of compound (3) on (a) gastrointestinal system, (b) kidney, (c) liver, (d) lungs, (e) blood, and (f) cardiovascular system. These maps illustrate the role of the individual atoms and fragments of the ligands in a color-coded manner; red color indicates a positive contribution to the toxicity whereas green color indicates the atom/fragment has no relevant effect.

micromole) and medium lethal concentration (LC$_{50}$ 1.8 mg/l) was predicted only in case of water flea (*Daphnia magna*) as aquatic toxicity. It is to be suggested that before going to start *in vivo* or any other advanced study, it is better to do *in vitro* and *in silico* analysis one more times of all data for confirming the best ligand.

## 4. Conclusion

In this study, comparatively better and reliable 3D homology model of DmTβH was performed. Docking studies of 1-[4-(trifluromethyl)phenyl]-1,3-dihydro-2*H*-imidazole-2-thione (3) into the active site of DmTβH resulted in lowest binding energy signifying highest binding affinity. The computational ADME and toxicity analysis established its drug-likeness and no predicted health hazard. In summary, it can be suggestid that this study will be advantageous in founding a base regarding the appropriate modeling of DmTβH and development of an effective and safe pesticide.

## Conflict of interest

The authors declare no conflict of interest.

## Acknowledgements

## References

1. Downer RGH: Trehalose production in isolated fat body of the American cockroach, *Periplaneta americana*. Comp Biochem Physiol, 62: 31-34, 1979.
2. Huddart H, Oldfield AC: Spontaneous activity of foregut and hindgut visceral muscle of the locust, *Locusta migratoria*. II. The effect of biogenic amines. Comp Biochem Physiol, 73: 303-311,1982.
3. Mcclung C, Hirsh J: The trace amine tyramine is essential for sensitization to cocaine in *Drosophila*. Curr Biol, 9: 853-860,1999.
4. Kutsukake M, Komatsu A, Yamamoto D, Ishiwa-Chigusa S: A tyramine receptor gene mutation causes a defective olfactory behavior in Drosophila melanogaster. Gene, 245: 31-42, 2000.
5. Nagaya Y, Kutsukake M, Chigusa SI, Komatsu A: A trace amine, tyramine functions as a neuromodulator in *Drosophila melanogaster*. Neurosci Lett, 329: 324-328, 2002.
6. Sasaki K, Nagao T: Distribution and level of dopamine and its metabolites in brains of reproductive workers in honeybees. J Insect Physiol, 47: 1205-1216, 2002.
7. Blumenthal EM: Regulation of chloride permeability by endogenously produced Tyramine in the *Drosophila Malpighian* tubule. American J Physiology-cell and Physiol, 284: 718-728, 2003.
8. Donini A, Lange AB: Evidence for a possible neurotransmitter /neuromodulator role of tyramine on the locust oviducts. J Insect Physiol, 50: 351-361, 2004.
9. Saraswati S, Fox LE, Soll DR, Wu CF: Tyramine and octopamine have opposite effects on the locomotion of *Drosophila* larvae. J Neurobiol, 58: 425-441, 2004.
10. Long TF, Edgecomb RS, Murdock, LL: Effects of substituted phenylethylamines on blowfly feeding behavior. Comp Biochem Physiol, 83: 201-209, 1986.
11. Goosey MW, Candy DJ: The D-octopamine content of the haemolymph of the locust, *Schistocerca gregaria* and its elevation during flight. Insect Biochem, 10: 393-397, 1980.
12. Orchard I, Lange AB: Evidence for octopaminergic modulation of an insect visceral muscle. J Neurobiol, 16: 171-181. 1985.
13. Lee HG, Seong CS, Kim, YC, Davis RL, Han KA: Octopamine receptor OAMB is required for ovulation in *Drosophila melanogaster*. Dev Biol, 264: 179-190, 2003.
14. Monastirioti M: Distinct octopamine cell population residing in the CNS abdominal ganglion controls ovulation in *Drosophila melanogaster*. Dev Biol, 264: 38-49, 2003.
15. Dudai Y: cAMP and learning in *Drosophila*. Adv Cyc Nucl Prot Phosph Res, 20: 343-361, 1986.
16. Yovell Y, Dudai Y: Possible involvement of adenylate cyclase in learning and short-term memory. Experimental data and some theoretical consider-

ations. Isr J Med Sci, 23: 49-60, 1987.

17. Hirashima A, Yamaji H, Yoshizawa T, Kuwano E, Eto M: Effect of tyramine and stress on sex-pheromone production in the pre- and post-mating silkworm moth. J Insect Physiol, 53: 1242-1249, 2007.

18. Nathanson JA: Octopamine receptors, adenosine-3', 5'-monophosphate and neural control of firefly flashing. Science, 203: 65-68,1979.

19. Orchard I, Ramirez JM, Lange AB: A multifunctional role for octopamine in locust flight. Annu Rev Entomol, 38: 227-249, 1993.

20. Barron AB, Schulz DJ, Robinson GE: Octopamine modulates responsiveness to foraging-related stimuli in honey bees (*Apis mellifera*). J Comp Physiol A, 188: 603-610, 2002.

21. Tang YL, Epstein MP, Anderson GM, Zabetian CP, Cubells JF: Genotypic and haplotypic associations of the DBH gene with plasma dopamine beta hydroxylase activity in Africans Americans. Eur J Hum Genet, 15: 878-883, 2007.

22. James R, McCarthy, Donald P, et al: 1-(Thienylalkyl) imidazole-2 (3H)-thiones as potent competitive inhibitors of dopamine. beta.-hydroxylase. J Med Chem, 33: 71866-1873,1990.

23. Hirashima A, Matsushita M, Ohta O, Nakazono K, Kuwano E, Eto M: Prevention of progeny formation in *Drosophila melanogaster* by 1-arylimidazole-2-(3*H*)-thiones. Pestic Biochem Physiol, 85: 15-20, 2006.

24. Kruse I, Kaiser C, DeWolf WE Jr, et al.: Multisubstrate inhibitors of dopamine beta-hydroxylase. 1. Some 1-phenyl and 1-phenyl-bridged derivatives of imidazole-2-thione. J Med Chem, 29: 2465-2472, 1986.

25. McGinnis S, Madden TL: BLAST: at the core of a powerful and diverse set of sequence analysis tools. Nucleic Acids Res, 32: W20-25, 2004.

26. Dereeper A, Guignon V, Blanc G, et al.: Phylogeny fr.: robust phylogenetic analysis for the non-specialist. Nucl Acids Res, 36: W 465-469, 2008.

27. Dereeper A, Audic S, Claverie JM, Blanc G: Blast-EXPLORER helps you building datasets for phylogene analysis. BMC Evol Biol, 10: 8, 2010.

28. Sali A, Potterton L, Yuan F, van Vlijmen H, Karplus M. Evaluation of comparative protein modeling by MODELLER. Proteins, 23: 318-326, 1995.

29. Maestro- Schrödinger release 2016-1: Combiguide (version 4.0), Schrödinger, LLC, New York, NY, 2016.

30. Laskowski RA, Rullmann JAC, MacArthur MW, Kaptein R, Thornton JM: AQUA and PROCHECK-NMR: programs for checking the quality of protein structures solved by NMR. J Biomol NMR, 8: 477-486,1996.

31. Arnold K, Bordoli L, Kopp J, Schwede T: The SWISS-MODEL workspace: a web-based environment for protein structure homology modeling. Bioinformatics. 22: 195-201, 2006.

32. Trott O, Olson AJ: AutoDock Vina: improving the speed and accuracy of docking with a new scoring function, efficient optimization and multithreading. J Comput Chem, 31: 455-461, 2010.

33. Altschul SF, Madden TL, Schaffer AA, et al.: Gapped BLAST and PSI-BLAST: a new generation of protein database search programs. Nucleic Acids Res, 25: 3389-3402, 1997.

34. Sali A, Blundell TL: Comparative protein modeling by satisfaction of spatial restraints. J Mol Biol, 234: 779-815, 1993.

35. Dundas J, Ouyang Z, Tseng J, Binkowski J, Turpaz Y, Liang J: CASTp: computed at as of surface topography of proteins with structural and topographical mapping of functionally annotated residues. Nucl. Acids Res, 34: W116-118, 2006.

36. Liang J, Edelsbrunner H, Woodward C: Anatomy of Protein Pockets and Cavities: Measurement of Binding Site Geometry and Implications for Ligand Design Protein Sci, 7: 1884-1897, 1998.

37. Lipinski CA, Lombardo F, Dominy BW, Feeney PJ: Experimental and computational approaches to estimate solubility and permeability in drug discovery and development settings. Adv Drug Deliv Rev, 23: 4-25, 1997.